SAKARYA ÜNİVERSİTESİ
FEN BİLİMLERİ ENSTİTÜSÜ DERGİSİ

Sakarya University Journal of Science
SAUJS

e-ISSN 2147-835X Period Bimonthly Founded 1997 Publisher Sakarya University
http://www.saujs.sakarya.edu.tr/

Title: A Numerical Investigation for the Effect of Environmental Conditions on the Bending Behavior of Laminated Composites

Authors: Rabi Ezgi BOZKURT, Fatih DARICIK

Recieved: 2021-04-21 00:00:00

Accepted: 2022-02-17 00:00:00

Article Type: Research Article

Volume: 26
Issue: 2
Month: April
Year: 2022
Pages: 249-261

How to cite
Rabi Ezgi BOZKURT, Fatih DARICIK; (2022), A Numerical Investigation for the Effect of Environmental Conditions on the Bending Behavior of Laminated Composites. Sakarya University Journal of Science, 26(2), 249-261, DOI: 10.16984/saufenbilder.925144
Access link
https://dergipark.org.tr/tr/journal/1115/issue/69580/925144

Sakarya University Journal of Science 26(2), 249-261, 2022

A Numerical Investigation for the Effect of Environmental Conditions on the Bending Behavior of Laminated Composites

Rabi Ezgi BOZKURT[1], Fatih DARICIK*[1]

Abstract

In this study, the bending behavior of fiber-reinforced laminated composites (FRCs) with a balanced and symmetric stacking sequence was investigated numerically under different environmental conditions. The numerical models of carbon/ bismaleimide, carbon/epoxy, and S-glass/epoxy laminated composites were designed and analyzed using ESAComp software. Deformation of the FRCs models was simulated with three-point bending conditions and the effects of material properties varying with environmental conditions on the flexural analysis were investigated according to the Tsai-Wu criterion and the Puck criterion. The Tsai-Wu criterion detects the failure of FRCs earlier and behaves more conservative than the Puck criterion for all environmental conditions. The flexural strength and failure mode of the laminates vary with the variation of environmental conditions. The order of the first damaged ply varied depending on the type of reinforcing fiber. Especially the presence of moisture and high temperature significantly influences the flexural strength of the laminated composites.

Keywords: Laminated composites, environmental conditions, three-point bending, failure analysis

1. INTRODUCTION

FRCs are very attractive because of their superior specific strength properties. FRCs are used in many engineering applications that contain different loads, such as static, fatigue, hygrothermal, etc. The fibers supply high strength and rigidity for in-plane properties of the FRCs. Out-of-plane properties of the FRCs are depending on the strength of matrix materials which are lower than that of the reinforcing fibers. The hygrothermal stability of the polymer matrix materials is also very low according to the fibers. Thus, the environmental conditions and thermal/hygrothermal aging directly affect the mechanical strength of the FCRS [1-5]. The surface treatment of the reinforcing material is another factor that can vary the mechanical behavior of the FCRs by changing the interface strength of the matrix and fibers [6], [7]. In recent years, studies have been carried out to increase the strength of the FCRs by strengthening them with nanoparticles [8-13]. Türkmen et al. produced glass fiber mat reinforced composite materials that have a different number of layers by the using hand lay-up method [14]. The three-point bending test method was used to determine the flexural strength of GFRP materials. Because of the test,

* Corresponding author: fatih.daricik@alanya.edu.tr
[1] Alanya Alaaddin Keykubat University, Rafet Kayış Faculty of Engineering, Machine Engineering Department
E-mail: ezgibozkurt80@gmail.com
ORCID: https://orcid.org/0000-0002-7714-1819, https://orcid.org/0000-0002-5813-1260

the maximum bending strength of 150.85 MPa was got from the manufactured materials. Bingöl et al. compared the flexural properties of glass mat reinforced composites and the woven glass fiber reinforced composite materials [15]. The research results showed that the higher fiber length of the non-woven fiberglass fabric provides higher flexural strength and the bending strength of woven glass fiber reinforced composite material is higher than that of the non-woven fiberglass fabric reinforced composites.

The physical and mechanical properties of fiber-reinforced composite materials can be improved by adding various additives. Gülşah et al investigated the flexural strength of E-glass fiber/epoxy composite materials with carbon nanotube added [16]. The experimental results have shown the addition of %0.75w carbon nanotube increased the flexural modulus and the flexural strength of the material in a ratio of %36 and %23, respectively. Kıratlı et al. reported that the graphene nanoplatelets significantly increased the flexural strength of the E-glass/epoxy laminated composites [13]. Hybrid composite structures are attracted nowadays, as many different fiber types can be used as reinforcement elements. Aydın et al. have manufactured glass fabric reinforced, carbon fabric reinforced, and hybrid glass/carbon fabric reinforced laminates and compared the flexural properties of the laminates [17]. The study presented that just carbon fiber reinforced composite structure exhibits maximum bending strength among the tested laminates.

Metal plate reinforced hybrid materials can be shown high mechanical properties. Bellini et al. investigated the flexural strength and fracture behavior of different types of aluminum carbon fibers [18]. Experimental results showed that the presence of an aluminum sheet provides an increment of the flexural strength and a slight decrease of the required energy to propagation of the crack. Furthermore, the presence of the adhesive at the composite/metal interface made the flexural strength decrease and the fracture energy increase.

The hybridization of natural fibers with their superior aging resistance and synthetic fibers relevant attention in terms of environmental impact and the durability they are provided. Calabrese et al. glass-flax/epoxy hybrid composites materials were exposed to salt–fog environmental conditions for up to 60 aging days [2]. They evidenced that adding glass fibers in flax layers positive affected flexural strength and modulus can be observed. Laminated composite materials with high fiber angles are more prone to stress concentration on the layers. Reis et al. studied stress relaxation behavior of glass/polyamide-6 composites considering different fiber directions [1], as well as exposure to NaOH and HCl solutions. Consequently, compared with the laminates with fibers at 0◦, flexural strength decreased approximately up to 50%, respectively, for the orientations of 30◦ and 45◦.

Fiber, matrix, adhesive and interface components in composite material are susceptible to degradation of Ph changed. Wang et al. GFRP composite material has been exposed to salt-water and water [3]. Consequently, the degradation was faster in saltwater than in tap water. Also, when the exposure time was increased, there has been a serious decreased in the strain values. Harrison et al. presented that seawater reduces the flexural strength of carbon/epoxy and glass/epoxy composite materials in the long term [4]. Pavan et al. showed the bending strength and damage formation of GFRP laminates composite materials under different environmental conditions [19]. They evidenced that the bending strength decreases with increasing exposure temperature. Bazli et al. investigated the flexural strength of GFRP laminated composite material under different temperature conditions [20]. Conclusion reported that as the thickness of the composite materials decreases, the flexural strength decreases when the exposure time at high temperatures increases. Meng et al. examined the CFRP from 77 K° to 298 K° and showed that the flexural strength increased as the cryogenic temperature decreased [21]. Also, has been shown that the cryogenic temperature affects the durability of the matrix and the failure mode of the layers.

In the literature examined, it has been observed that different environmental conditions affect the flexural strength of the materials. Depended on the changing environmental conditions, the change in strength values can be determined by three-point bending analysis. In this paper, Carbon fiber/bismaleimide, carbon fiber/epoxy and S-glass fiber/epoxy layered composite materials are designed with balanced symmetry and angled storied. These materials have been examined for their flexural behavior under different environmental conditions. The deformation caused by the bending load in FRC materials was investigated using the Tsai-Wu and Puck failure criteria.

2. MATERIAL AND METHOD

Three-point bending analyses were done by simulating the real test according to ASTM D790. Three different reinforced plies were considered to design FRC laminates and then to perform flexural analysis. Carbon fiber/bismaleimide (Cytek_CB) unidirectional ply, carbon fiber/epoxy (Toray_CE) unidirectional ply, and S-glass fiber/epoxy (Cytek_S-GE) unidirectional ply was employed with the material property sets that differed according to environmental conditions (Table 1). The ambient temperature 24℃ was assume as the reference for all the materials. The weight amount of moisture in the ambient was also expressed as +w%, i.e., 82℃+1w%. The laminates were designed with the symmetric and balanced stacking sequence of $[0_n/30_n/\text{-}30_n/60_n/\text{-}60_n/90_n]_s$ via ESAComp software (Figure 1). The subscript *n* is equal to 3 for 36 layers of Cytek_CB, 2 for 24 layers of Toray_CE, and 1 for 14 layers of Cytek_S-GE. However, there is an exception for Cytek_S-GE that the subscript *n* is 2 for the 0° reinforced layer. As a result of selected stacking sequences, the thicknesses of the laminates (*d*) Cytek_CB, Toray_CE, and Cytek_S-GE were 3.37 mm, 3.65 mm, and 3.30 mm respectively. The geometrical models of the three-point bending specimen were prepared with dimensions of 60 mm in the length (*L*) and 12.67 mm in the width (*b*) (Figure 2). Each laminate with different material property sets has been investigated for flexural behavior.

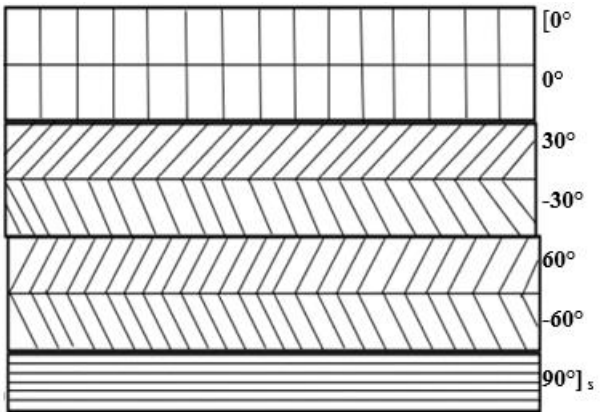

Figure 1 Stacking sequence of the laminates

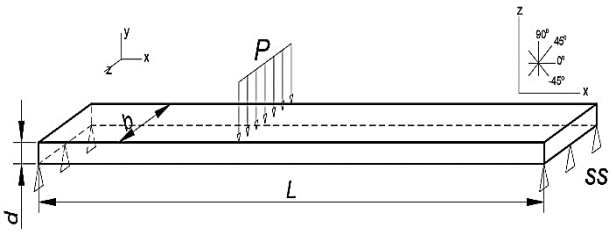

Figure 2 The dimensions of the model for bending analysis

Table 1 Mechanical Properties of FRCs Materials [22-24]

Symbol		Cytek_CB (ρ =1.568g/cm^3 V_f=60%)			Cytek_S-GE (ρ =1.839g/cm^3 V_f=49%)					Toray_CE (ρ =1.555g/cm^3 V_f=55%)			
Cond.	Temp. (°C)	-55	24	177	-54	24	66	82	82	-54	24	82	82
	Moist. (%)	0	0	1	0	0	1	0	1	0	0	0	1
Elastic Properties	E_1 (GPa)	169.00	160.00	138.00	48.81	47.99	47.13	46.88	47.37	121.00	119.00	121.00	119.50
	E_2 (GPa)	10.35	9.70	9.00	15.79	15.79	12.31	13.20	11.51	52.98	9.00	7.50	7.00
	E_3 (GPa)	10.35	9.70	9.00	15.79	15.79	12.31	13.20	11.51	52.98	9.00	7.50	7.00
	G_{12} (GPa)	5.90	5.90	2.00	4.27	4.07	3.72	3.72	2.62	5.00	4.00	4.00	3.00
	G_{31} (GPa)	5.90	5.90	2.00	4.27	4.07	3.72	3.72	2.62	5.00	4.00	4.00	3.00
	G_{23} (GPa)	3.98	3.73	3.46	5.85	5.85	4.56	4.89	4.26	4.26	3.33	2.78	2.59
	υ_{12}	0.30	0.30	0.30	0.28	0.26	0.26	0.26	0.30	0.35	0.31	0.31	0.32
	υ_{13}	0.30	0.30	0.30	0.28	0.26	0.26	0.26	0.30	0.35	0.31	0.31	0.32
	υ_{23}	0.30	0.30	0.30	0.35	0.35	0.35	0.35	0.35	0.35	0.35	0.35	0.35
Stregth Properties	X_t (MPa)	2897.00	2618.00	2278.00	1274.79	1501.20	934.52	1418.18	880.74	1682.01	2172.44	2206.66	2259.82
	Y_t (MPa)	63.00	66.00	28.00	56.54	56.54	56.40	59.64	49.71	52.98	48.86	44.23	25.91
	Z_t (MPa)	63.00	66.00	28.00	56.54	56.54	56.40	59.64	49.71	52.98	48.86	44.23	25.91
	X_c (MPa)	1620.00	1620.00	966.00	1240.16	1179.76	951.55	508.21	688.92	1396.50	1449.77	1410.32	1199.97
	Y_c (MPa)	207.00	194.00	180.00	274.27	274.27	185.68	208.57	165.13	282.44	198.67	147.72	116.43
	Z_c (MPa)	207.00	194.00	180.00	274.27	274.27	185.68	208.57	165.13	282.44	198.67	147.72	116.43
	S_{12} (MPa)	102.00	103.00	77.00	169.96	132.17	96.73	103.01	81.84	159.52	154.74	128.31	95.22
	S_{31} (MPa)	102.00	103.00	77.00	169.96	132.17	96.73	103.01	81.84	159.52	154.74	128.31	95.22
	S_{23} (MPa)	59.71	55.96	51.92	87.72	87.72	68.37	73.35	63.97	63.89	50.00	41.67	38.89

The numerical models of the bending specimens were prepared with rectangular shell elements. Longer edges of the model were divided into 120 parts and the aspect ratio for the elements was adjusted to 1. Boundary conditions for the shorter edges were set as free along the *z*-direction, as fixed along the *y*-direction. The translation of the edges along the *x*-direction was kept at *x=0* and released at *x=L*. Rotations around all of the directions were released too. Thus, the ratio of the support span to the thickness was approximately 20:1 for all the models. Then the models were loaded along the *y*-direction with a centered line load. The models were loaded until the failure was detected. In the numerical model, the value of the load causing failure was recorded.

The failure of the modeled composite materials under bending load was determined according to both the Tsai-Wu and the Puck failure criteria. According to the Tsai-Wu failure criterion, if the *f* value calculated with Equation 1is less than 1 so that the composite material is safe. The load value that makes the *f* value equal to or less than 1 was taken as failure load (P_{cr}) and the corresponding deflection (δ_{cr}) was recorded. In Equation 1, the σ_1 and σ_2 express the axial stresses along the reinforcement direction (direction-*1*) and transverse direction (direction-*2*). The term τ_{12} expresses the shear stress on the *1-2* plane. Other coefficients are the constants dependent on the material strength (Table 1).

$$f = F_1\sigma_1 + F_2\sigma_2 + F_6\tau_{12} + 2F_{12}\sigma_1\sigma_2 + F_{11}\sigma_1^2 + F_{22}\sigma_2^2 + F_{66}\tau_{12}^2 \quad (1)$$

$$F_1 = \frac{1}{X_t} - \frac{1}{X_c}, \quad F_2 = \frac{1}{Y_t} - \frac{1}{Y_c}, \quad F_6 = 0 \quad (2)$$

$$F_{11} = \frac{1}{X_t X_c}, \quad F_{22} = \frac{1}{Y_t Y_c}, \quad F_{66} = \frac{1}{S^2} \quad (3)$$

The Puck criterion dissociates the damage of the laminates into reinforcement failure (*FF*) and matrix material failure (*MF*). The criterion uses the indices *IFF* and *IMF* for fiber failure and

matrix failure, respectively. According to the criterion, reinforcement fiber failure occurs only under tensile load in the direction of the fiber and the matrix material failure is handled with three different fracture modes (Figure 3). According to Mode A failure, matrix fracture occurs on a plane parallel to the reinforcing fibers due to tensile forces transverse to the reinforcing direction. In Mode B failure, matrix fracture occurs between reinforcing fibers in the material under shear stresses and small compressive stresses. In Mode C failure, matrix cracks occur along inclined planes in the material under compression loads. Equations 4-10 are used to control each failure mode.

$$\sigma_1 > 0 \rightarrow I_{FF} = \sigma_1 / F_{1t} \tag{4}$$

$$-\sigma_1 < 0 \rightarrow I_{FF} = -\sigma_1 / F_{1c} \tag{5}$$

$$\sigma_2 \geq 0 \rightarrow$$

$$I_{MF,A} = \sqrt{\left(\frac{\sigma_6}{F_6}\right)^2 + \left(1 - p_{6t}\frac{F_{2t}}{F_6}\right)^2 \left(\frac{\sigma_2}{F_{2t}}\right)^2} + p_{6t}\frac{\sigma_2}{F_6} \tag{6}$$

$$\left.\begin{matrix} \sigma_2 < 0 \\ \left|\frac{\sigma_2}{\sigma_6}\right| \leq \frac{F_{2A}}{F_{6A}} \end{matrix}\right\} \rightarrow$$

$$I_{MF,B} = \frac{1}{F_6}\left[\sqrt{\sigma_6^2 + (p_{6c}\sigma_2)^2} + p_{6c}\sigma_2\right] \tag{7}$$

$$F_{2A} = \frac{F_6}{2p_{6c}}\left[\sqrt{1 + 2p_{6c}\frac{F_{2c}}{F_6}} - 1\right] \tag{8}$$

$$p_{2c} = p_{6c}\frac{F_{2A}}{F_6} \tag{9}$$

$$\left.\begin{matrix} \sigma_2 < 0 \\ \left|\frac{\sigma_2}{\sigma_6}\right| \leq \frac{F_{2A}}{F_{6A}} \end{matrix}\right\} \rightarrow$$

$$I_{MF,C} = -\frac{F_{2c}}{\sigma_2}\left[\left(\frac{\sigma_6}{2(1+p_{2c})F_6}\right)^2 + \left(\frac{\sigma_2}{F_{2c}}\right)^2\right] \tag{10}$$

According to Puck and Schürmann (2004), stress and strain analysis, failure criterion, and strength degradation of each layer of laminate are required to form the most realistic failure envelope [25]. However, the researchers neglected the reduced strength values that emerged with the first failure of layered composite materials under load in the failure criterion they proposed. For the failure analysis of the laminates with the Tsai-Wu and Puck criteria, when just one ply of the laminates was damaged then the entire laminates were assumed as damaged. This approach is called first ply failure (*FPF*).

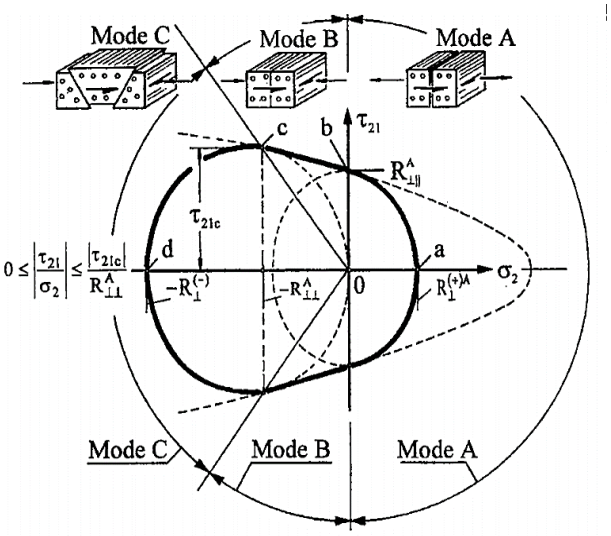

Figure 3 Formation of damage modes A, B, and C under plane stress σ_2 and τ_{21} according to the Puck criterion [24]

3. RESULT

3.1. Analysis of carbon/ bismaleimide/ composites

Variations of the P_{cr} and δ_{cr} for Cytek_CB were presented in Figures 4-5. According to both of the Tsai-Wu and Puck criteria, the bending strength of the Cytek_CB at room temperature (the reference material) is maximum, and it is slightly lower at -55°C. However, the bending strength of the Cytek_CB has been drastically reduced with the increase in temperature and the presence of moisture in the environment. According to the Tsai-Wu criterion, the bending strength of the Cytek_CB at -55°C and 177°C+1.15w% is respectively 3.61% and 57.39% lower than that of the reference material. According to the Puck criterion, the bending strength of the Cytek_CB at -55°C and 177°C+1.15w% is respectively 3.58% and 53.3% lower than that of the reference material.

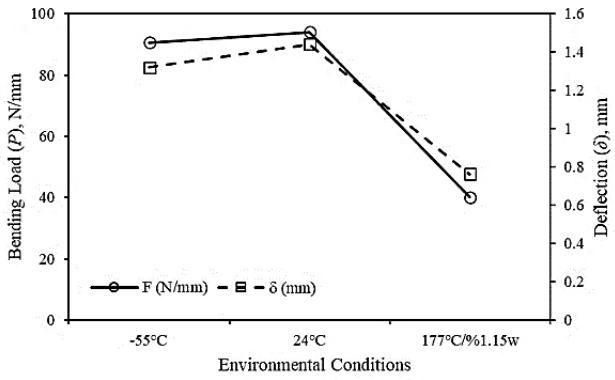

Figure 3 P_{cr} and δ_{cr} values of the Cytek_CB by the Tsai-Wu criterion

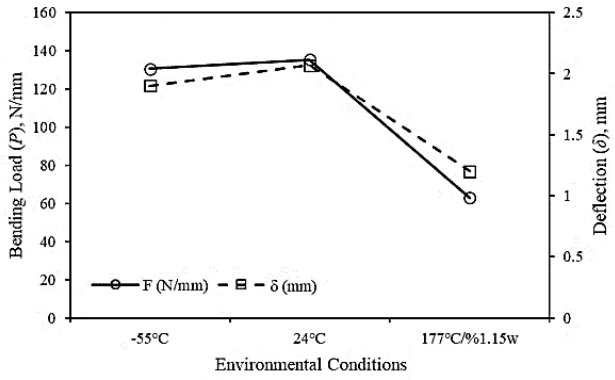

Figure 4 P_{cr} and δ_{cr} values of the Cytek_CB by the Puck criterion

The ply-wise stress (σ_1) distributions in the reference material along the fiber direction because of the P_{cr} were presented and compared (Figures 6-7). The variation of σ_1 has similar characteristics for all the environmental conditions according to both the Tsai-Wu and Puck criteria. Because of bending load, the longitudinal compressive stresses on the upper part, according to the mid plane, caused tensile σ_1 in the layers with 60°, -60°, and 90° reinforcements. The arrangement of the layers is balanced and symmetrical, so the stress distribution across the thickness of the layers is symmetric concerning the midplane.

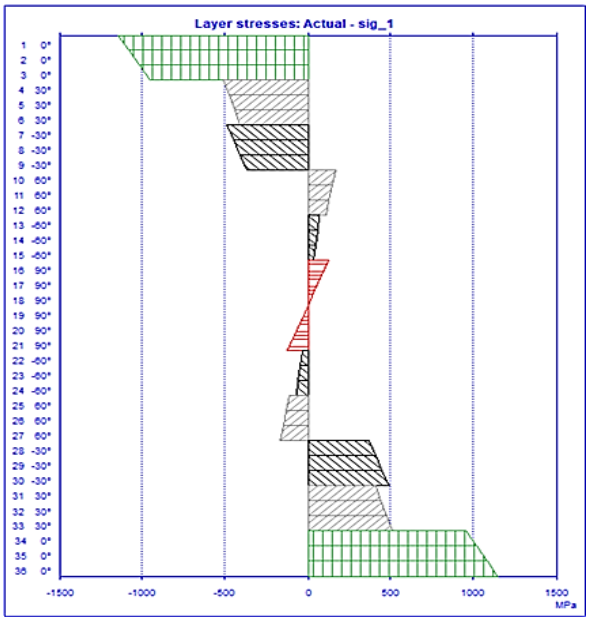

Figure 5 σ_1 values at room temperature for the Cytek_CB by the Tsai-Wu criterion

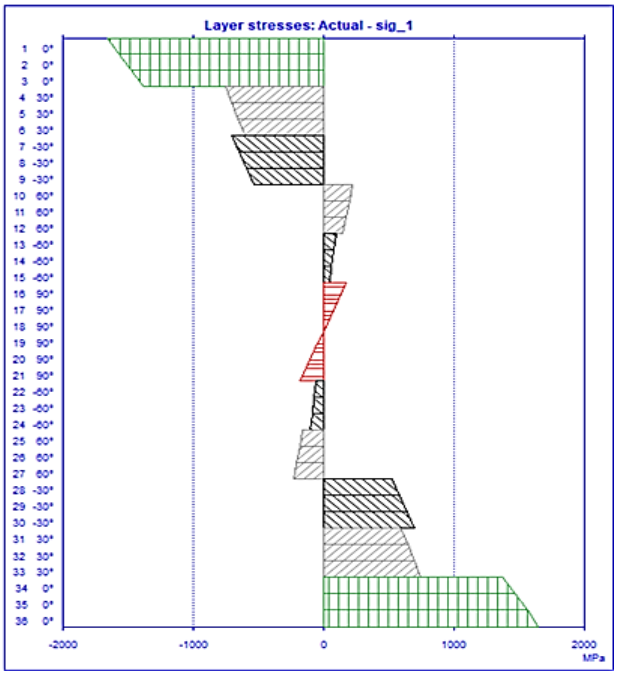

Figure 6 σ_1 values at room temperature for the Cytek_CB by the Puck criterion

The maximum stresses have occurred as tensile at 36th ply and as compression in the first layer. With the bending load applied to the Cytek_CB, the top layer has been damaged first. According to the Puck criterion, it has been observed that the damage mode is Mode A which comprises fiber failure compression (*ffc*) and planar shear stress. On the other hand, the damage is caused because

of transverse tensile (*2t*) stress, according to Tsai-Wu. The detected failure modes were valid for the failures under all environmental conditions except for the Tsai-Wu result of 177°C+1.15w%. Inverse reserve factor (*IRF*) values calculated by Tsai-Wu and Puck criterion for each layer of Cytek_CB material at room temperature has given in Figures 8-9, respectively. Because of failure loads, the Tsai-Wu criterion detects the failure of Cytek_CB early and behaves more conservative than the Puck criterion for all environmental conditions.

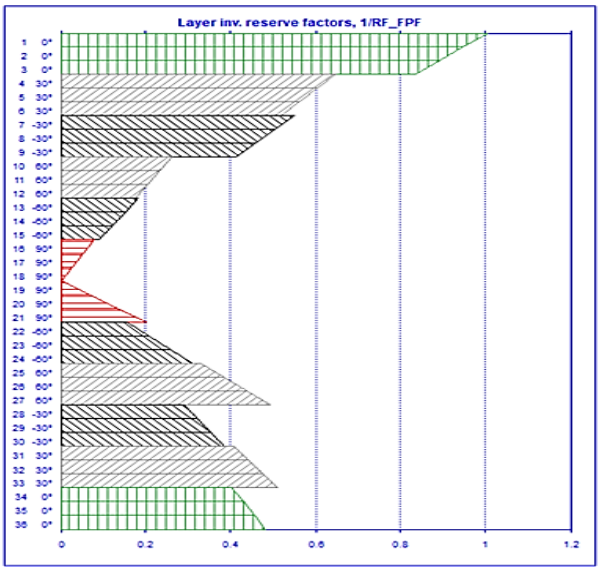

Figure 7 IRF values of the Cytek_CB layers by the Tsai-Wu Criterion

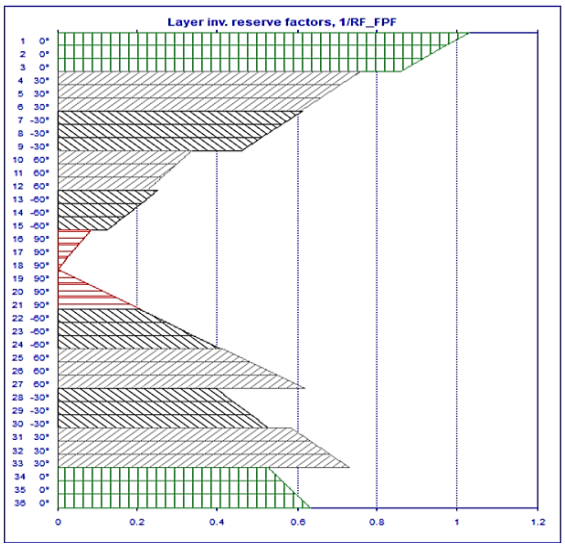

Figure 8 IRF values of the Cytek_CB layers by the Puck criterion

3.2. Analysis of carbon /epoxy / composites

P_{cr} and δ_{cr} variations for the Toray_CE in different environmental conditions were presented in Figure 10-11. According to both of the Tsai-Wu and Puck criteria, the bending strength of the Toray_CE is maximum at 82°C and it is slightly lower at -54°C and 24°C. Furthermore, the flexural strength of Toray_CE was decreased significantly with the increase in temperature and the presence of moisture. According to the Tsai-Wu criterion, the flexural strength of Toray_CE increased by 3.7% when the temperature decreased from the reference condition (room temperature) to -54°C and decreased 0.18% when it increased to 82 °C. Also, the flexural strength of Toray_CE was significantly reduced by 31.02% at the condition 82°C+1w% compared to the reference Toray_CE. According to the Puck criterion, the flexural strength of the Toray_CE increased by 2.2% when the temperature decreased from the reference condition to -54°C and decreased 0.4% when it increased to 82°C. Also, the flexural strength of Toray_CE was significantly reduced by 28.6% at the condition 82°C+1w% compared to the reference Toray_CE.

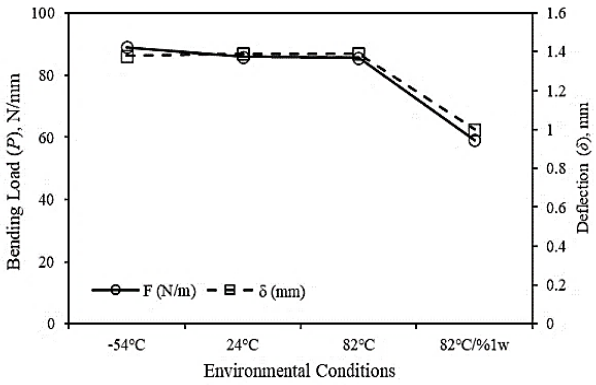

Figure 9 P_{cr} and δ_{cr} values of the Toray_CE by the Tsai-Wu criterion

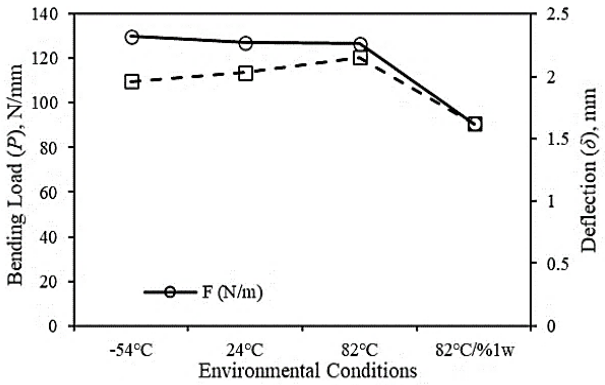

Figure 10 P_{cr} and δ_{cr} values of the Toray_CE by the Puck criterion

The ply-wise σ_1 distributions in the reference material along the fiber direction because of P_{cr} were presented in Figures 12-13. Although the planar tensile and compression strength of Cytek_CB is higher compared to Toray_CE, the flexural strength of Toray_CE is higher. This may be because of the higher shear strength of Toray_CE. The σ_1 distributions given for the Tsai-Wu and Puck damage criteria at room temperature showed similar results for all conditions. Because of bending load, the longitudinal compressive stresses on the upper part according to the mid-plane caused tensile σ_1 in the layers with 60°, -60°, and 90° reinforcements.

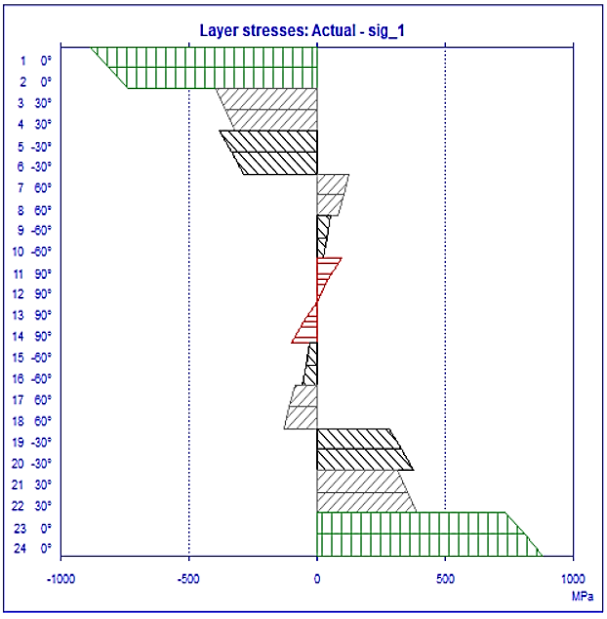

Figure 11 σ_1 values at room temperature for the Toray_CE by the Tsai-Wu criterion

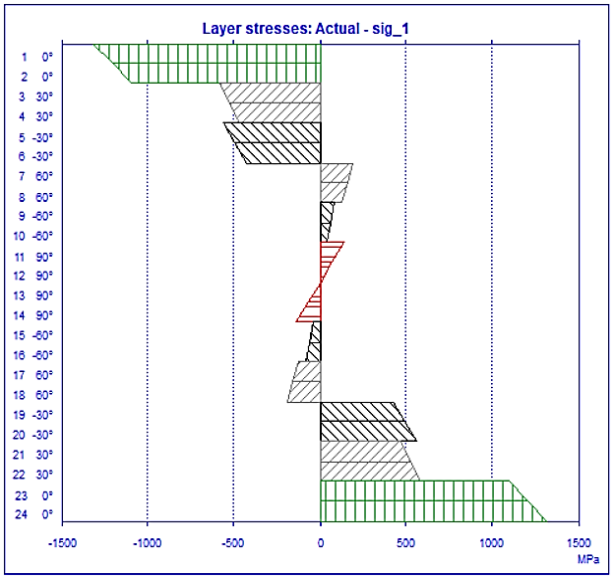

Figure 12 σ_1 values at room temperature for the Toray_CE by the Puck criterion

The maximum stresses have occurred as tensile at 24th ply and as compression in the first layer. With the bending load applied to the Toray_CE material, the top layer has been damaged first. According to the Puck criterion, it has been observed that the damage mode is Mode A. The detected failure modes according to the Puck criterion were valid for the failures of the materials under all environmental conditions. On the other hand, failure modes according to Tsai-Wu criterion could be just compression along the fiber direction (*1c*), transverse tensile (*2t*), and the combination of the first two failure modes (*1c/2t*). IRF values calculated by Tsai-Wu and Puck criterion for each layer of Toray_CE material at room temperature has given in Figures 14-15, respectively. As a result of failure loads, the Tsai-Wu criterion detects the failure of Toray_CE early and behaves more conservative than the Puck criterion for all environmental conditions.

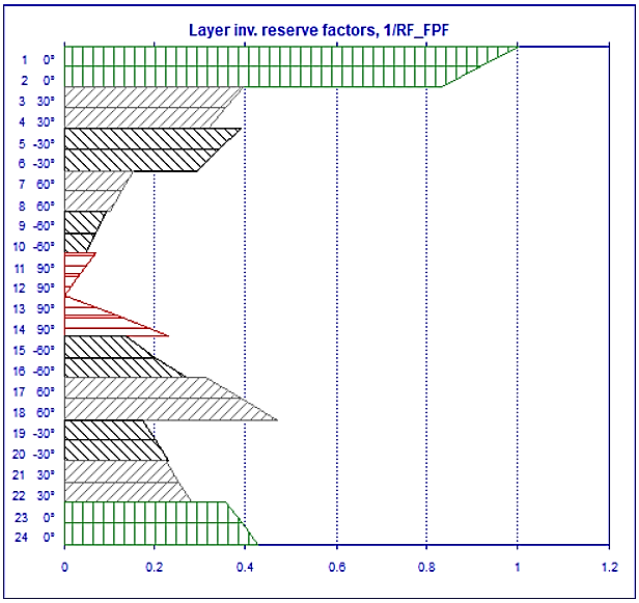

Figure 13 IRF values of the Toray_CE layers by the Tsai-Wu Criterion

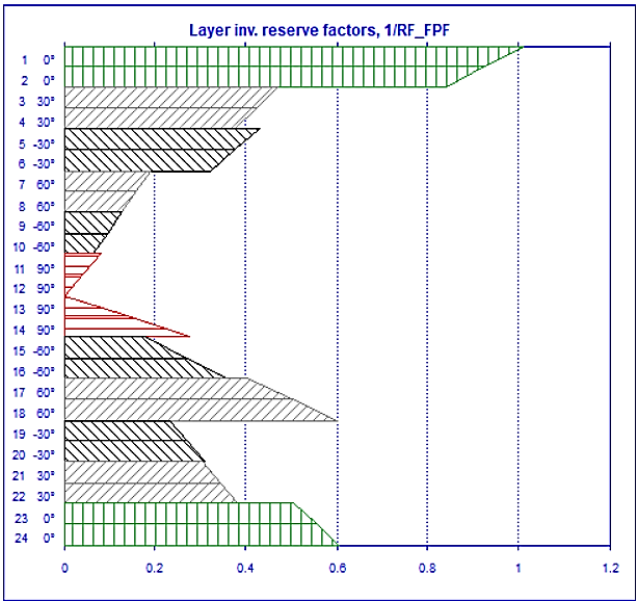

Figure 14 IRF values of the Toray_CE layers by the Puck criterion

3.3. Analysis of S-glass/epoxy/composites

For Cytek_S-GE, variations of the P_{cr} and δcr due to environmental conditions were presented in Figure 16-17. According to both of the Tsai-Wu and Puck criteria, the bending strength of the Cytek_S-GE is maximum at 66°C+0.8w%. According to the Tsai-Wu criterion, the flexural strength of Cytek_S-GE increased by 3.15% when the temperature decreased from the reference condition (room temperature) to -54 °C and decreased 0.17% when it increased to 82 °C. Besides, the flexural strength of the Cytek_S-GE increased by 15.8% at the condition of 66°C+0.8w% and decreased by 15.44% at 82°C compared to reference Cytek_S-GE. According to the puck criterion, when the temperature increased to 82°C and decreased to -54°C, the flexural strength increased by 0.83% and 14.4%, respectively compared to reference Cytek_S-GE. The flexural strength of the material at 66°C+0.8w% is 16.8% higher than the strength of reference Cytek_S-GE and it is 13.6% lower at 82°C than the reference.

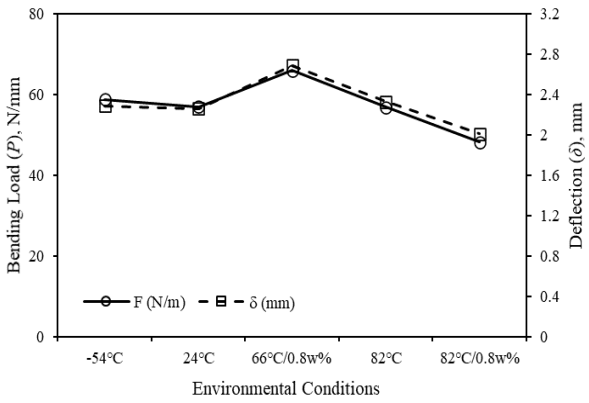

Figure 15 P_{cr} and δ_{cr} values of the Cytec_S-GE by the Tsai-Wu criterion

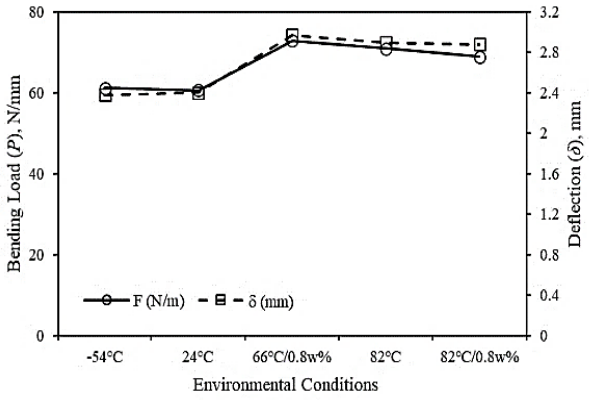

Figure 16 P_{cr} and δ_{cr} values of the Cytec_S-GE by the Puck criterion

The ply-wise σ_1 distributions in the reference material along the fiber direction due to P_{cr} were presented in Figures 18-19. The σ_1 distributions given for the Tsai-Wu and Puck damage criteria at room temperature showed similar characteristics for all conditions. Because of that,

the level of the 5th ply reinforced is just 0.24 mm higher than the 6th ply, the σ_1 at the 5th ply is tensile while the σ_1 6th ply is compressive. In addition to this, the tensile σ_1 comes up in the 90° reinforced layer on the mid-plane.

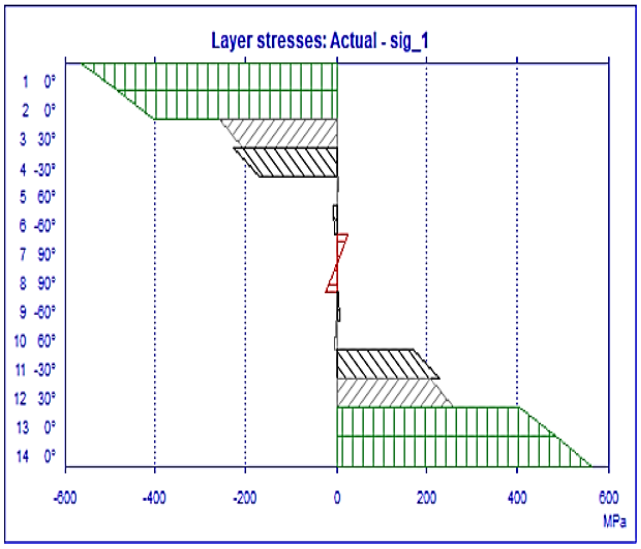

Figure 17 σ_1 values at room temperature for Cytec_S-GE by the Tsai-Wu criterion

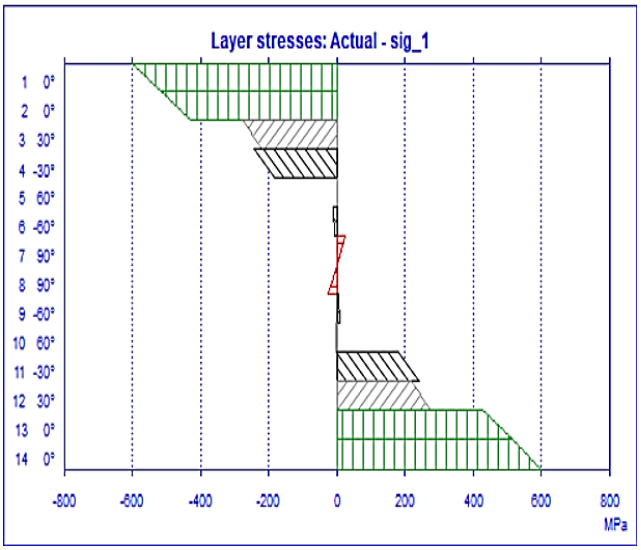

Figure 18 σ_1 values at room temperature for Cytec_S-GE by the Puck criterion

The maximum stresses have emerged as tensile at 14th ply and as compression in the first layer. With the bending load applied to the Cytek_S-GE, the 10th layer was damaged first. According to the Puck criterion, for all environmental conditions, it was observed that the damage mode is Mode A which comprises inter-fiber failure (*iff*) and planar shear stress. Also, the damage of reference material is caused by transverse tensile (*2t*) stresses according to Tsai-Wu. According to the Tsai-Wu criterion, the environmental conditions change the failure of materials. IRF values calculated by Tsai-Wu and Puck criterion for each layer of Cytek_S-GE material at room temperature were given in Figures 20-21, respectively. As a result of failure loads, the Tsai-Wu criterion detects the failure of Cytek_S-GE early and behaves more conservative than the Puck criterion for all environmental conditions.

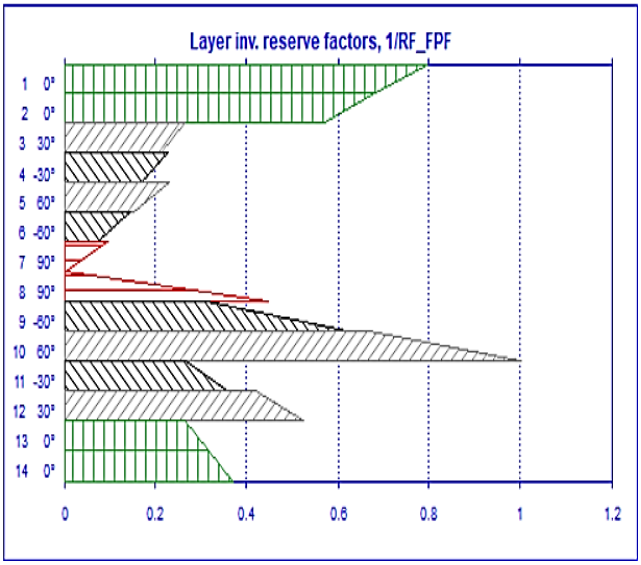

Figure 19 IRF values of the layers of the Cytec_S-GE by the Tsai-Wu Criterion

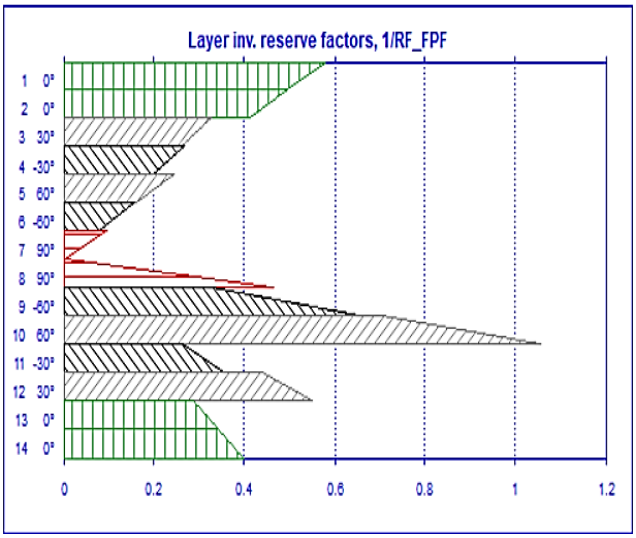

Figure 20 IRF values of the layers of the Cytec_S-GE by the Puck criterion

4. CONCLUSIONS

Numerical bending analyses of carbon/bismaleimide, carbon/epoxy, and S-glass/epoxy laminated composites were performed using ESAComp software. Materials property sets differing from environmental conditions were used for the analysis. Failure of the laminates was determined by the Tsai-Wu criterion and the Puck criterion. As a result of the analysis, the following conclusions have been obtained;

- The Tsai-Wu criterion detects the failure of FRCs earlier and behaves more conservative than the Puck criterion for all environmental conditions.
- The top layers where the line load directly affect, were damaged first in the Cytek_CB and Toray_CE laminated composites. Besides, the 10^{th} layer was damaged first in the Cytek_S-GE laminated composites.
- The variation of flexural strength differs according to the type of the laminated composite. However, high environmental temperature and moisture reduce the flexural strength.
- While the environmental conditions do not affect the damage mode according to the Puck criterion, the damage mode can change with the change of environmental conditions according to the Tsai-Wu criterion.

Funding

The authors have no received any financial support for the research, authorship, or publication of this study.

The Declaration of Conflict of Interest/ Common Interest

No conflict of interest or common interest has been declared by the authors.

Authors' Contribution

The authors contributed equally to the study.

The Declaration of Ethics Committee Approval

This study does not require ethics committee permission or any special permission.

The Declaration of Research and Publication Ethics

The authors of the paper declare that they comply with the scientific, ethical, and quotation rules of SAUJS in all processes of the paper and that they do not make any falsification of the data collected. In addition, they declare that Sakarya University Journal of Science and its editorial board have no responsibility for any ethical violations that may be encountered and that this study has not been evaluated in any academic publication environment other than Sakarya University Journal of Science.

REFERENCES

[1] A. M. Amaro, P. N. B. Reis, and M. A. Neto, “Experimental study of temperature effects on composite laminates subjected to multi-impacts,” Compos. Part B Eng., vol. 98, pp. 23–29, 2016.

[2] L. Calabrese, V. Fiore, T. Scalici, and A. Valenza, “Experimental assessment of the improved properties during aging of flax/glass hybrid composite laminates for marine applications,” J. Appl. Polym. Sci., vol. 136, no. 14, pp. 1–12, 2019.

[3] J. Wang, H. GangaRao, R. Liang, D. Zhou, W. Liu, and Y. Fang, “Durability of glass fiber-reinforced polymer composites under the combined effects of moisture and sustained loads,” J. Reinf. Plast. Compos., vol. 34, no. 21, pp. 1739–1754, 2015.

[4] P. Ghabezi and N. Harrison, “Mechanical behavior and long-term life prediction of carbon / epoxy and glass / epoxy composite laminates under artificial seawater environment,” Mater. Lett., p. 127091, 2019.

[5] F. Daricik and S. Kiratli, “Farklı Çevresel Ş artlarda İki Eksenli Yüklemelere Maruz

Tabakalı Kompozit Malzemelerin Hasarı Damage of Laminated Composite Materials Exposed to Biaxial Loads in Different," vol. 36, no. March, pp. 219–233, 2021.

[6] P. Kiss, J. Glinz, W. Stadlbauer, C. Burgstaller, and V. Archodoulaki, "The effect of thermally desized carbon fibre reinforcement on the flexural and impact properties of PA6 , PPS and PEEK composite laminates : A comparative study," Compos. Part B, vol. 215, no. March, p. 108844, 2021.

[7] P. Kiss, J. Schoefer, W. Stadlbauer, C. Burgstaller, and V. M. Archodoulaki, "An experimental study of glass fibre roving sizings and yarn finishes in high-performance GF-PA6 and GF-PPS composite laminates," Compos. Part B Eng., vol. 204, no. October 2020, p. 108487, 2021.

[8] C. L. Chiang, H. Y. Chou, and M. Y. Shen, "Effect of environmental aging on mechanical properties of graphene nanoplatelet/nanocarbon aerogel hybrid-reinforced epoxy/carbon fiber composite laminates," Compos. Part A Appl. Sci. Manuf., vol. 130, no. November 2019, p. 105718, 2020.

[9] A. Ramesh, K. Ramu, M. A. Ali Baig, and E. D. Guptha, "Influence of fly ash nano filler on the tensile and flexural properties of novel hybrid epoxy nano-composites," Mater. Today Proc., vol. 27, pp. 1252–1257, 2020.

[10] A. K. Srivastava, V. Gupta, C. S. Yerramalli, and A. Singh, "Flexural strength enhancement in carbon-fiber epoxy composites through graphene nano-platelets coating on fibers," Compos. Part B Eng., vol. 179, no. August, p. 107539, 2019.

[11] F. Daricik and A. Topcu, "Theoretical Analysis on the Thermal and Electrical Properties of Fiber Reinforced Laminates Modified with CNTs Karbon Nanotüp ile Modifiye Edilmiş Fiber Takviyeli Laminelerin Isıl ve Elektriksel Özelliklerinin Teorik Analizi," vol. 35, no. December, pp. 925–936, 2020.

[12] R. Keshavarz, H. Aghamohammadi, and R. Eslami-Farsani, "The effect of graphene nanoplatelets on the flexural properties of fiber metal laminates under marine environmental conditions," Int. J. Adhes. Adhes., vol. 103, no. August, p. 102709, 2020.

[13] S. Kıratlı and Z. Aslan, "Flexural Behavior of Graphene Nanoplatelets Reinforced Cross-Ply E- glass/epoxy Laminated Composite Materials Sakine," Cumhur. Sci. J., vol. 39, no. 2, pp. 531–542, 2018.

[14] I. Türkmen and N. S. Köksal "Investigation of mechanical properties and impact strength depending on the number of fiber layers in glass fiber," vol. 2, pp. 17–30, 2013.

[15] M. Bingöl and K. Çavdar, "Effects of Different Reinforcements for Improving Mechanical Properties of Composite Materials," Uludağ Univ. J. Fac. Eng., vol. 21, no. 2, p. 123, 2016.

[16] G. Öner, H. Y. Ünal, and Y. Pekbey, "Karbon nanotüp katkılı camlifi -epoksi kompozitlerin termal ve eğilme özelliklerinin araştırılması," no. 232, pp. 805–816, 2017.

[17] M. R. Aydın, V. Acar, F. Yapıcı, K. Yıldız, M. V. Topcu and Ö. Gündoğdu, "Influence of Fiber Stacking Sequence in Inter-ply Hybrid Composites Structures on the Mechanical and Dynamics Properties," vol. 8, no. 3, pp. 255–263, 2018.

[18] V. Di Cocco, F. Iacoviello, and L. Sorrentino, "Failure energy and strength of Al / CFRP hybrid laminates under flexural load," no. October, pp. 1–6, 2019.

[19] G. Pavan, K. K. Singh, and Mahesh, "Elevated thermal conditioning effect on flexural strength of GFRP laminates: An

experimental and statistical approach," Mater. Today Commun., vol. 26, no. November 2020, p. 101809, 2020.

[20] M. Bazli, H. Ashrafi, A. Jafari, X. L. Zhao, H. Gholipour, and A. V. Oskouei, "Effect of thickness and reinforcement configuration on flexural and impact behaviour of GFRP laminates after exposure to elevated temperatures," Compos. Part B Eng., vol. 157, pp. 76–99, 2019.

[21] J. Meng et al., "Mechanical properties and internal microdefects evolution of carbon fiber reinforced polymer composites : Cryogenic temperature and thermocycling effects," Compos. Sci. Technol., vol. 191, no. November 2019, p. 108083, 2020.

[22] Solvay Technical Data Sheet Cycom® 381 Prepreg 2021. https://catalogservice.solvay.com/downloadDocument?fileId=MDkwMTY2OWM4MDU1YmZmNg==&fileName=CYCOM381_CM_EN.pdf&base=FAST

[23] J. Tomblin, J. Mckenna, Y. Ng, and K. S. Raju, "Advanced General Aviation Transport Experiments B – Basis Design Allowables for Epoxy – Based Prepreg Fiberite 8-Harness Graphite Fabric," 2001.

[24] J. Tomblin, J. Sherraden, W. Seneviratne, and K. S. Raju, "A - Basis and B - Basis Design Allowables for Epoxy Based Prepreg," 2002.

[25] A. Puck and H. Schürmann, "Failure analysis of FRP laminates by means of physically based phenomenological models," Compos. Sci. Technol., vol. 62, no. 12-13 SPECIAL ISSUE, pp. 1633–1662, 2002.